SUPPLEMENTARY INFORMATION

Structure of the Integrin αIIb Transmembrane Segment

Tong-Lay Lau, Varun Dua and Tobias S. Ulmer

Department of Biochemistry & Molecular Biology and Zilkha Neurogenetic Institute, Keck School of Medicine, University of Southern California, 1501 San Pablo Street, Los Angeles, CA 90033

TABLE OF CONTENTS

Supplemental Table 1. Structural statistics for the αIIb transmembrane segment[a]

R.m.s. deviations from experimental dihedral restraints (deg)	
All *(69)*[b]	0.32 ± 0.14
R.m.s. deviations from experimental residual dipolar couplings (Hz)[c]	
$^{1}D_{NH}$ *(28)*	0.65 ± 0.02
$^{1}D_{NC'}$ *(27)*	0.63 ± 0.04
$^{1}D_{C\alpha C'}$ *(28)*	0.76 ± 0.06
R.m.s. deviations from experimental distance restraints (Å)	
All (*240*)	0.08 ± 0.01
Intraresidue (*81*)	0.04 ± 0.01
Interresidue sequential ($\|i - j\| = 1$) (*69*)	0.07 ± 0.01
Interresidue short range ($1 < \|i - j\| < 5$) (*78*)	0.12 ± 0.01
Interresidue long range ($\|i - j\| \geq 5$) (*12*)	0.07 ± 0.01
Deviations from idealized covalent geometry	
Bonds (Å)	0.004 ± 0.000
Angles (deg)	0.587 ± 0.020
Impropers (deg)	0.475 ± 0.014
Coordinate precision (Å)[d]	
Backbone non-hydrogen atoms	0.22
All non-hydrogen atoms	0.87
Measures of structural quality	
E_{LJ} (kcal mol^{-1})[3] [e]	-127.9
Residues in most favorable region of Ramachandran plot [f]	95.8%

A, Statistics for the 20 calculated simulated annealing structures, encompassing residues Ile966-Lys994.

B, Torsion angle restraints included 29 ϕ, 29 ψ, and 11 χ_1 angles.

C, R.m.s. deviations are normalized to an alignment tensor magnitude of 10 Hz.

D, Defined as the average r.m.s. difference between the final 20 simulated annealing structures and the mean coordinates.

E, The Lennard–Jones van der Waals energy was calculated with the CHARMM PARAM 19/20 parameters and was not included in the simulated annealing target function.

F, PROCHECK V3.4.4 (Roman A. Laskowski, Malcolm W. MacArthur, David S. Moss and Janet M. Thornton (1993). PROCHECK: a program to check the stereochemical quality of protein structures. J. Appl. Cryst., 26, 283-291)

Supplemental Table 2. χ_1 rotamer distribution of bicelle-embedded αIIb.

residue	$^3J_{C'C\gamma}$	$^3J_{NC\gamma}$	type	chi1	flag[a,b]
966	5.65	-	ILE	-	-
967	3.09	0.04	TRP	-60	loose
968	4.67	0.01	TRP	-60	tight
969	4.06	1.96	VAL	-	averaged
970	3.38	1.22	LEU	-	averaged
971	3.97	2.13	VAL	-	averaged
973	4.63	1.96	VAL	-	averaged
974	3.01	0.62	LEU	-60	loose
978	3.44	1.55	LEU	-	averaged
979	3.65	1.28	LEU	-60	loose
980	3.94	1.41	LEU	-60	loose
981	2.46	1.97	THR	-	averaged
982	4.09	2	ILE	-	averaged
983	2.79	1.37	LEU	-	averaged
984	3.81	2.04	VAL	-	averaged
985	3.56	0.79	LEU	-60	tight
987	5.1	0.84	MET	-60	tight
988	0.01	2.68	TRP	180	tight
989	0.55	1.6	LYS	180	loose
990	1.74	1.23	VAL	-	averaged
992	1.51	1.39	PHE	-	averaged
993	3.54	0.65	PHE	-60	tight
994	4.64	1.17	LYS	-60	loose

a, In the present case, a tightly defined rotameric state is considered for $^3J_{NC\gamma}$ in either *trans* (2.4 ± 0.6 Hz) or *gauche* (≤0.8 Hz) conformation and $^3J_{C'C\gamma}$ in either *trans* (4.0 ± 0.6 Hz) or *gauche* (≤1.1 Hz) conformation. Loosely coupled states are considered for $^3J_{NC\gamma}$ in either *trans* (2.4 ± 0.9 Hz) or *gauche* (≤1.0 Hz) conformation and $^3J_{C'C\gamma}$ in either *trans* (4.0 ± 1.0 Hz) or *gauche* (≤1.7 Hz) conformation. In case of borderline values additional combinations are also considered.

b, For all averaged rotamers, the most probable rotameric state has been selected (c.f. Experimental Procedures).

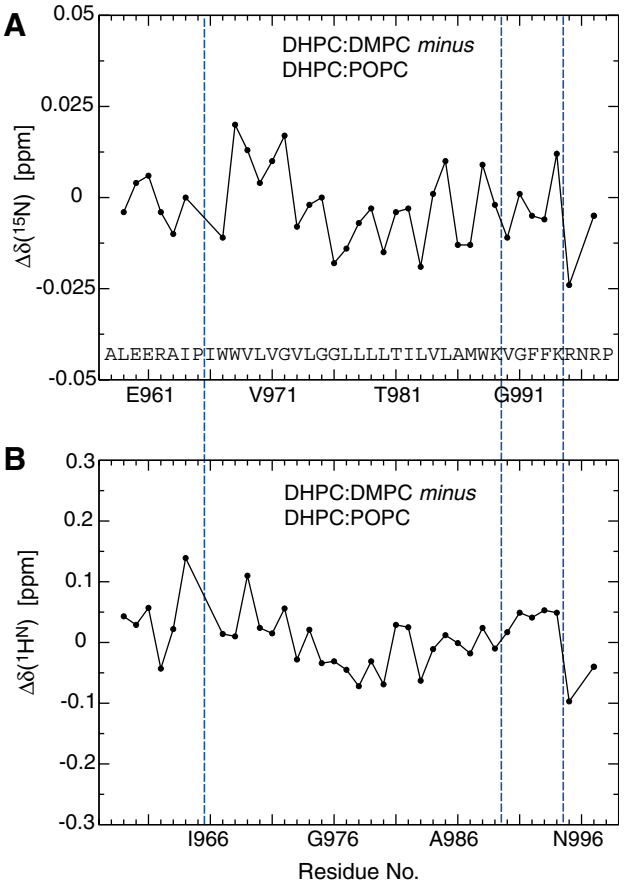

Supplemental Figure 1. Effect of lipid hydrocarbon chain length on αIIb chemical shifts. H-N chemical shifts differences between bicelles utilizing POPC (1-Palmitoyl-2-Oleoyl-*sn*-Glycero-3-Phosphocholine) and DMPC (1,2-Dimyristoyl-*sn*-Glycero-3-Phosphocholine) as long-chain lipids, respectively. No significant chemical shifts differences are observed. Solution conditions were 105 mM long-chain lipids and 350 mM DHPC (1,2-Dihexanoyl-*sn*-Glycero-3-Phosphocholine), 25 mM HEPES·NaOH, pH 7.4, 6% D_2O, 0.02% w/v NaN_3.

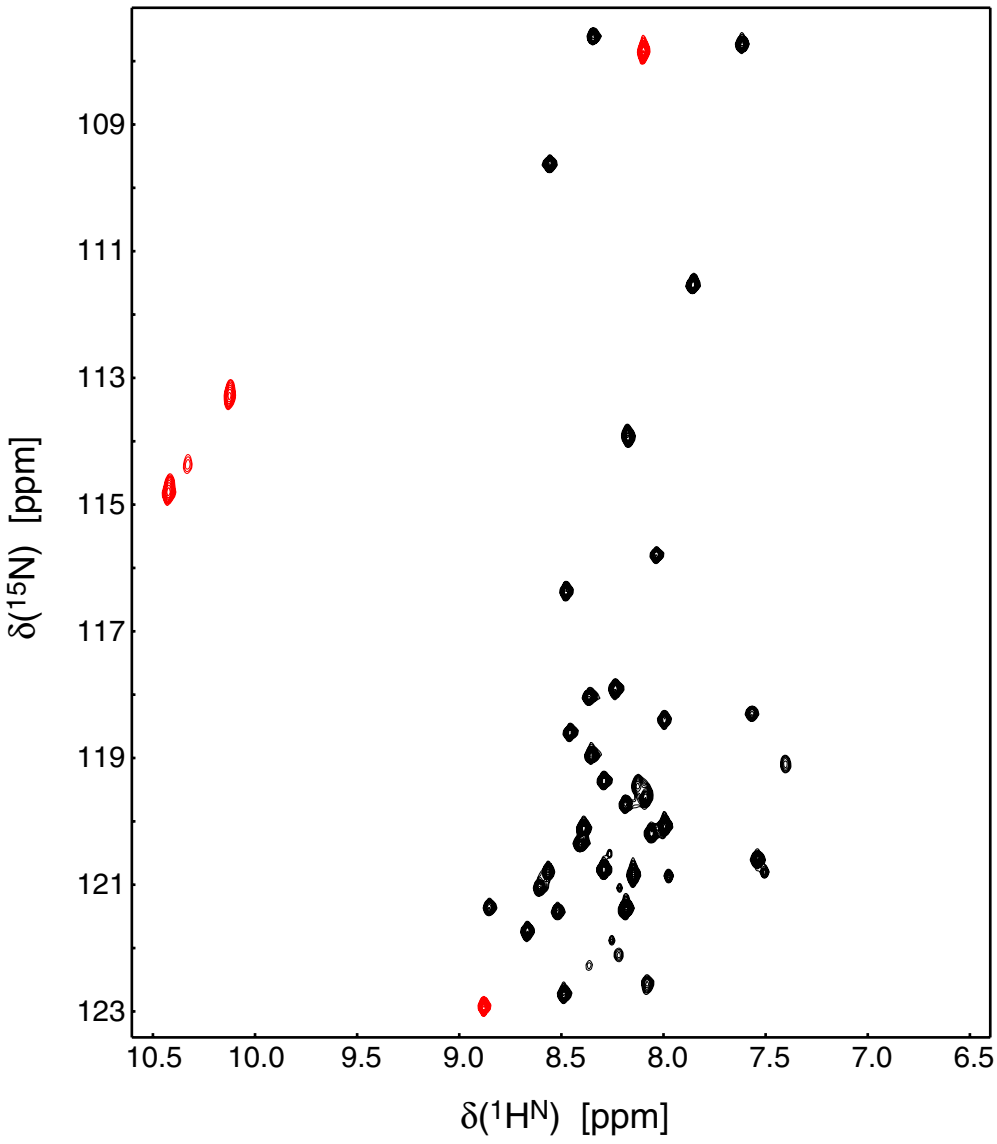

Supplemental Figure 2. H-N TROSY spectrum of bicelle-embedded αIIb. Bicelles consisted of 105 mM POPC (1-Palmitoyl-2-Oleoyl-*sn*-Glycero-3-Phosphocholine), 350 mM DHPC (1,2-Dihexanoyl-*sn*-Glycero-3-Phosphocholine) in 25 mM HEPES·NaOH, pH 7.4, 6% D_2O, 0.02% w/v NaN_3 solution. $^{2}H/^{13}C/^{15}N$ labeled αIIb peptide is present at ~0.6 mM. The spectrum was recorded at 35 °C and a ^{1}H frequency of 700 MHz.

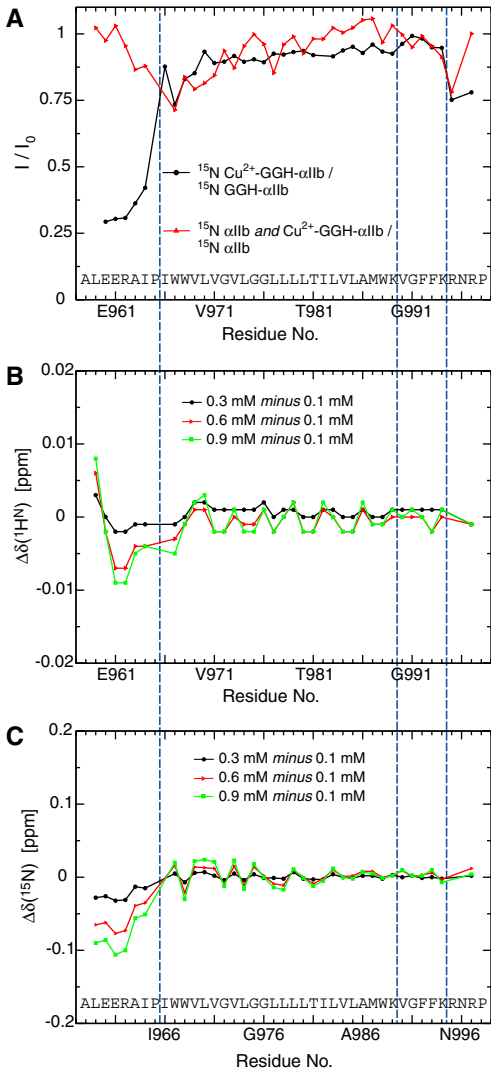

Supplemental Figure 3. Concentration dependence of αIIb spectral parameter. **A**, Transfer of paramagnetic relaxation enhancement from amino terminal Cu^{2+}-tagged αIIb peptides to untagged peptides. A high-affinity amino-terminal Gly957-Gly958-His959 Cu^{2+}-binding site was introduced, which substantially broadens the intensities of ^{15}N GGH-αIIb residues Glu960-I964, expressed as H-N TROSY signal intensity in the presence and absence of Cu^{2+}-loading, I/I_0. In contrast, no paramagnetic relaxation-induced broadening is transferred from 0.3 mM Cu^{2+}-GGH-αIIb to 0.3 mM ^{15}N αIIb peptides. Experiments were performed in 105 mM POPC, 350 mM DHPC, 25 mM HEPES·NaOH, pH 7.4, 6% D_2O, 0.02% w/v NaN_3 solution. **B-C**, Concentration dependence of αIIb $^1H^N$ and ^{15}N chemical shifts. Shift changes compared to 0.1 mM ^{15}N αIIb are plotted. The structured region (Ile966-Lys994) exhibits no significant shift changes. Very small shift changes are observed for the dynamically unstructured N-terminal residues, which may arise from increasing intermolecular collision at higher concentrations and/or minor differences in solution conditions between the samples. In contrast to the C-terminal residues, the N-terminal residues are more sensitive to changes in chemical environment (Fig. 2B-C). Shifts were measured in 105 mM POPC, 350 mM DHPC, 25 mM HEPES·NaOH, pH 7.4, 6% D_2O, 0.02% w/v NaN_3 solution. The transmembrane helix (I966-K989) borders and the Lys994-Arg995 transition are marked in all panels by blue lines.

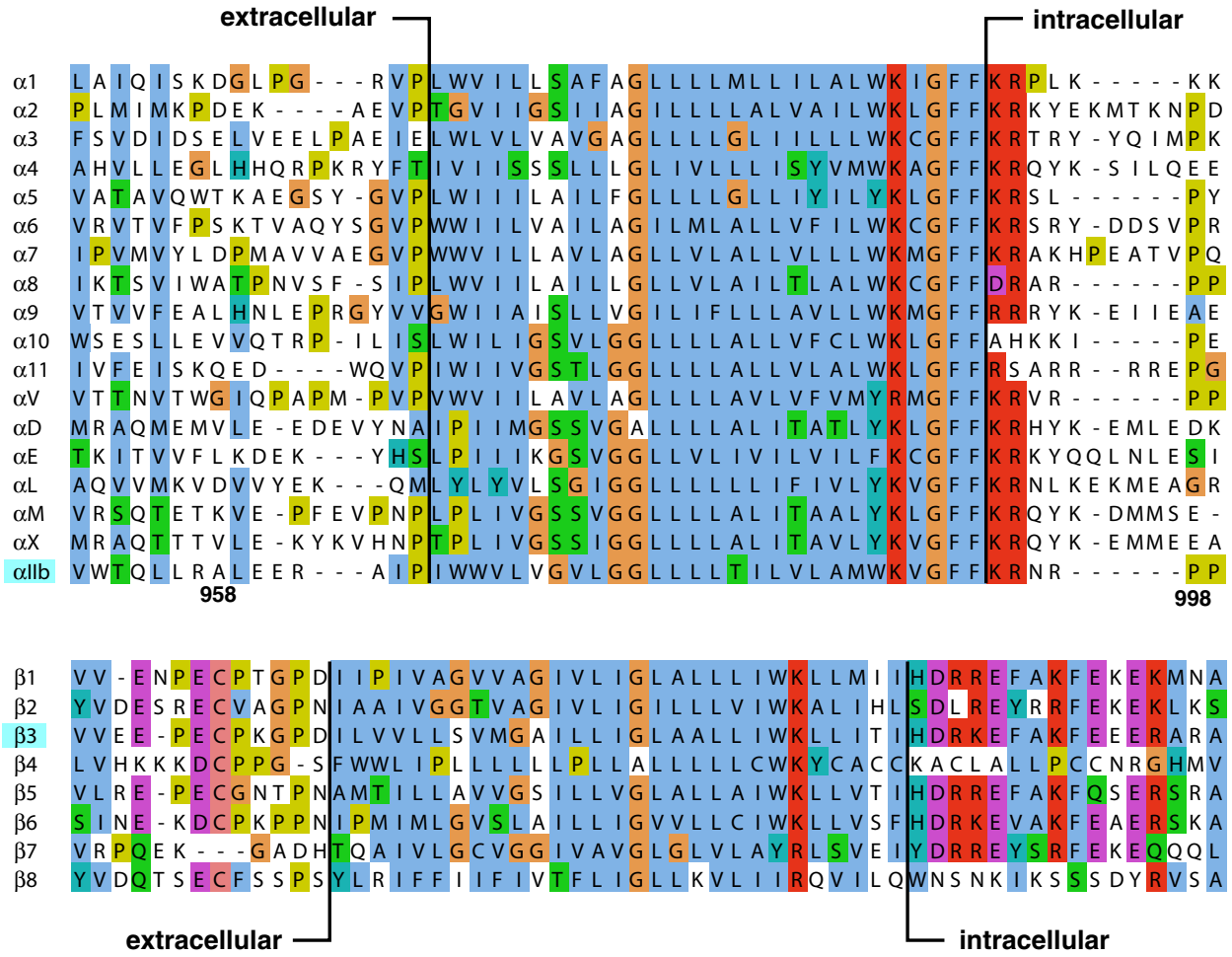

Supplemental Figure 4. Sequence alignment of all 18 human integrin α subunits and all 8 β subunits. Proposed minimal lipid tail-to-headgroup borders for monomeric α and β subunits are depicted. Conserved amino acids are colored by the jalview multiple alignment editor using the Clustalx color scheme.

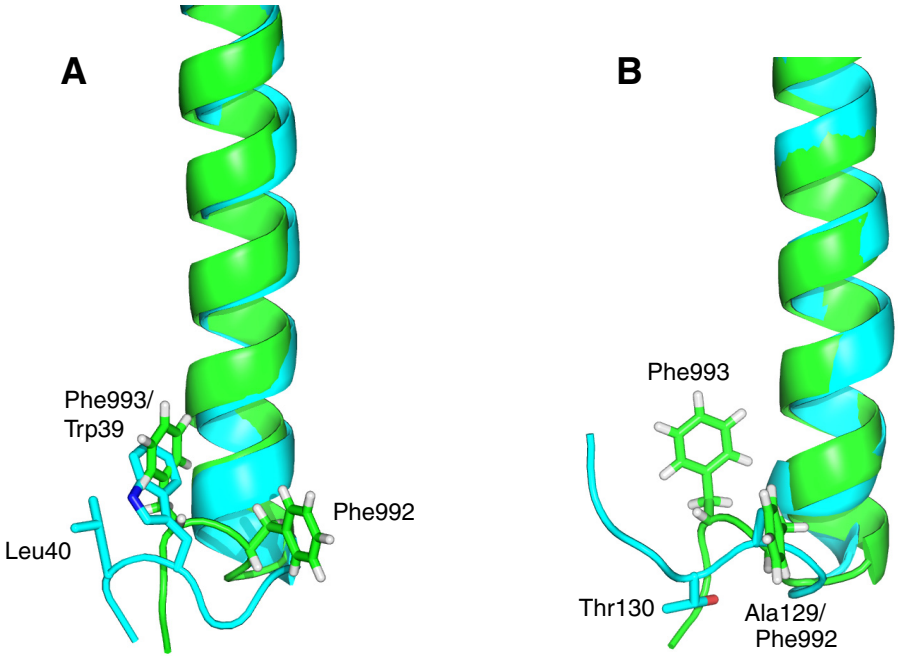

Supplemental Figure 5. Structural neighbors of the integrin αIIb TM segment. A close structural homology was found for a β peptide from the light-harvesting protein B-800/850, homologous PDB entries 2fkw (chain S), 1nkz (chain F) and 1kzu (chain B). Panel ***A***, shows the structural alignment of integrin αIIb(Pro965-Arg995), in *green*, with chain F of 1nkz, in *cyan*. The side chains of αIIb(Phe992-Phe993) and 1nkz-F(Trp39-Leu40) are shown in ball-and-stick representation. Phe993 and Trp39 are structurally homologous. A somewhat less close relative was found in cytochrome c oxidase, PDB entry 1xme (chain A), shown in *cyan* in panel ***B***. The side chains of αIIb(Phe992-Phe993) and 1xme-A(Ala129-Thr130) are shown in ball-and-stick representation. Phe992 and Ala129 are structurally homologous.